Düzce University
Journal of Science & Technology

Research Article

The Role of Self-Assembly Monolayers (SAM) on Schottky Diode Performance

Adem MUTLU [a,*], Cem TOZLU [b], Mustafa CAN [b]

[a] *Solar Energy Institute, Ege University, İzmir, TÜRKİYE*
[b] *Graphene Application and Research Center, İzmir Katip Celebi University, İzmir, TÜRKİYE*
* *Corresponding author's e-mail address: adem.mutlu@ege.edu.tr*

DOI: 10.29130/dubited.1530876

ABSTRACT

This study investigates the electrical and charge transport properties of Schottky diodes with a p-Si/TiO_2/SAM/Al structure, incorporating the self-assembly monolayers (SAMs) 4'', 4''''-[biphenyl-4,4''-diylbis(phenylimino)]dibiphenyl-4-carboxylic acid (MZ187) onto a titanium dioxide (TiO_2) layer synthesized via the sol-gel method. The impact of the MZ187 molecule on diode performance was evaluated based on parameters such as the barrier height ($\emptyset_b$), ideality factor (n), and series resistance (R_s). Experimental results reveal that the MZ187 monolayers on TiO_2 substantially enhanced diode performance, reducing the n from 3.7 for the control diode to 2.7 for the MZ187-modified diode. The R_s was also significantly reduced, while the $\emptyset_b$ increased. The rectification ratio increased from $1.3x10^2$ for the control diode to $2.2x10^3$ for the MZ187 modified diode. These improvements are attributed to the ability of MZ187 molecules to minimize interface states (N_{ss}) and improve surface quality. These findings underscore the critical role of SAMs in optimizing Schottky diode performance and demonstrate how the MZ187 molecule enhances diode efficiency by altering interface properties. The effectiveness of SAM coatings in enhancing Schottky diode performance makes a significant contribution to the field of nanoelectronics. This research paves the way for future studies on the use of SAMs in various nano electronic applications and offers promising potential for improving the performance and reliability of these technologies.

Keywords: *Schottky diode, sol-gel TiO_2, self-assembly monolayer, electrical characterization, interfaces, surface modification*

Kendiliğinden Organize Olan Tek Tabaka Moleküllerin (SAM) Schottky Diyot Performansı Üzerindeki Rolü

ÖZ

Bu çalışma, p-Si/TiO_2/SAM/Al yapısına sahip Schottky diyotlarının elektriksel ve yük taşıma özelliklerini incelemektedir. Schottky diyotları, sol-jel yöntemiyle sentezlenen titanyum dioksit (TiO_2) tabakasına, kendiliğinden organize olan monolayer (SAM) molekülü olan 4'',4'' ''-[bifenil-4,4'' -diylbis(fenilimino)]dibifenil-4-karboksilik asit (MZ187) uygulanarak üretilmiştir. MZ187 molekülünün diyot performansı üzerindeki etkisi, idealite faktörü (n), seri direnci (R_s) ve bariyer yüksekliği ($\emptyset_b$) gibi parametreler üzerinden değerlendirilmiştir. Deneysel sonuçlar, TiO_2 üzerinde monolayer MZ187 kaplamasının diyot performansını önemli ölçüde iyileştirdiğini göstermektedir. Kontrol diyot için 3.7

Received: 13/08/2024, Revised: 23/10/2024, Accepted: 30/10/2024

olan n, MZ187 modifiye diyot için 2.7'ye düşmüştür. R_s, MZ187 nedeniyle azalmış ve $\varnothing_b$ artmıştır. Doğrultma oranı, kontrol diyot için $1.3x10^2$'den MZ187 modifiye diyot için $2.2x10^3$'e yükselmiştir.
Bu iyileşmeler, MZ187 moleküllerinin arayüzey durumlarını (N_{ss}) minimize etme ve yüzey özelliklerini geliştirme yeteneğine atfedilmektedir. Bu çalışma, SAM'ların Schottky diyot performansını optimize etmedeki kritik rolünü vurgulamakta ve MZ187 molekülünün arayüzey özelliklerini değiştirerek diyot verimliliğini nasıl iyileştirdiğini göstermektedir. SAM kaplamalarının Schottky diyot performansını artırmadaki etkinliği, nanoelektronik alanına önemli katkılar sağlamaktadır. Bu araştırma, SAM'ların çeşitli nanoelektronik uygulamalarda kullanımına yönelik gelecekteki çalışmalara temel oluşturmakta ve bu teknolojilerin performansını ve güvenilirliğini artırmada umut verici etkiler sunmaktadır.

Anahtar Kelimeler: *Schottky diyot, sol-gel TiO_2, kendiliğinden organize olan tek tabaka, elektriksel karakterizasyon, arayüzeyler, yüzey modifikasyonu*

I. INTRODUCTION

Metal/insulator/semiconductor (MIS) contacts play a crucial role in semiconductor device technology and significantly influence the stability and performance of these devices. The behavior of these devices is determined by the characteristics of the semiconductor/metal interface. The insulating interface layer in MIS structures plays a critical role in enhancing device performance by affecting the barrier height ($\varnothing_b$) and diode parameters [1-4]. The performance of MIS Schottky diodes is influenced by various parameters such as the interface states at the insulator/metal and insulator/semiconductor interfaces, the $\varnothing_b$, the ideality factor (n), and the series resistance (R_s). Both the interface layer and R_s are critical parameters for MIS Schottky diodes because the total voltage applied to the diode is shared among the R_s, interface layer and the depletion layer. The magnitude of this voltage depends on the structure of the interface layer and thickness as well as R_s. Therefore, since the effectiveness and reliability of these devices are closely linked to both the R_s and the quality of the interface layer, it is imperative to meticulously account for R_s to achieve an accurate and reliable assessment of their electrical characteristics [5-9].

Titanium dioxide (TiO_2) is a widely studied material due to its impressive properties, such as a high dielectric constant, thermal stability, wide bandgap, high refractive index, and low leakage current density [10,11]. Considering its general properties, TiO_2 exhibits high transparency across a wide range of wavelengths due to the combination of Ti 3d and O 2p orbitals. Although TiO_2 has three different crystal phases—anatase, rutile, and brookite—all phases have the same chemical formula. However, differences in bond lengths and crystal structures among the phases lead to variations in density and electronic properties. The band gaps are 3.2 eV, 3.0 eV, and 3.3 eV for anatase, rutile and brookite respectively, resulting in distinct electronic properties for each phase [12]. While the anatase and rutile phases have similar valence band positions, brookite has a lower band position. The band positions vary among the phases, with brookite having the highest conduction band position. Anatase and rutile phases possess a tetragonal crystal system, whereas brookite has an orthorhombic structure. The surface properties also differ; anatase and rutile are more hydrophobic compared to brookite. The stability and efficiency of TiO_2 phases depend on nanoparticle size and synthesis method. Anatase is preferred for smaller nanoparticles, while rutile and brookite are stable at larger sizes [12-14]. The versatile nature of TiO_2 makes it promising for a wide range of applications, including catalysis, sensors, anti-reflective coatings, solar cells, and Schottky diodes. TiO_2 can be produced using various methods such as sol-gel technique, atomic layer deposition (ALD) and chemical vapor deposition, sputtering [15]. Among these techniques, the sol-gel method offers high control over the solution, ensuring control of composition and homogeneity. It also provides advantages over other coating approaches, particularly in situations where cost is a significant concern [16].
In 2008, Altındal et al. coated p-Si with TiO_2 prepared with the sol-gel method and coated with a dip-coating technique. They achieved n of 1.51 at room temperature and observed a significant decrease in the zero-bias barrier height ($\varnothing_{b0}$) along with an increase in the n value over the temperature range of 80-300 K [17]. Barış et al. used the DC magnetron sputtering technique to produce Au/TiO_2 (rutile) and

Au/TiO_2 (anatase) structures. They observed that as the temperature increased, the $\varnothing_b$ increased from 0.57 to 0.82 eV for rutile and increased from 0.74 to 0.85 eV for anatase [18,19]. In 2014, Aydın et al. achieved *n* of 1.8 and $\varnothing_b$ of 0.66 eV from Al/TiO_2/p-Si diodes prepared using the ALD [20]. In 2015, Altındal et al. reported $\varnothing_b$ of 1.068 eV at 100 kHz and 0.347 eV at 1 MHz in Au/TiO_2/n-4H-SiC diode structures prepared using the ALD [21]. In 2018, Yılmaz et al. achieved $\varnothing_b$ of 0.92 eV and *n* of 2.39 at room temperature from Ag/TiO_2 nanotube/Ti electrode structures containing TiO_2 nanotubes produced using the electrochemical anodization method [22]. In 2021, Taşdemir et al. reported *n* of 2.39 for Al/Zr-doped TiO_2/p-Si structures synthesized using sol-gel and drop-casting methods [23]. In 2022, Bilgili et al. achieved *n* of 1.39 and a $\varnothing_b$ of 0.52 eV for thin TiO_2 films, and *n* of 1.41 and $\varnothing_b$ of 0.50 eV for thick TiO_2 films in Ag/TiO_2/n-InP diode structures prepared using the sputtering method [24]. Tsui et al. demonstrated that coating the metal/4H-SiC interface with a 5 nm TiO_2 layer reduced the $\varnothing_b$ from 0.9 eV to 0.63 eV [25]. In 2023, Taşyürek coated TiO_2 nanotubes, produced using the anodization method, with DC magnetron sputtering to create Pt/TiO_2 nanotube/Ti diodes, achieving *n* of 1.25 and $\varnothing_b$ of 0.91 eV [26].

Surface states (N_{ss}) on semiconductor surfaces arise from defects, doped bonds, oxygen vacancies, structural changes due to metallization, doping atom levels, and natural or deposited interface layers at the metal/semiconductor interface. These conditions significantly impact the electrical parameters and conduction mechanisms of semiconductor devices. Reducing these conditions is critical for high-performance devices. TiO_2 is a commonly used insulating layer in Schottky diodes, as noted in many studies, and it contains surface defects that require passivation. While various methods exist to passivate defects in TiO_2, employing self-assembly monolayers (SAMs) provides a simpler and more cost-efficient approach to addressing surface defects [27-31].

SAMs are composed of three main components: head groups, alkyl chains, and functional groups. These structures chemically bond to surface atoms and arrange themselves in a two-dimensional pattern, improving surface morphology. This can lead to higher current densities and luminescence values in applications such as LEDs [32]. SAMs are widely used in various fields, including organic thin-film transistors (OTFTs), OLEDs, solar cells and nano sensors. They can also be used to reduce trap states caused by hydroxyl groups on SiO_2 substrates in silicon-based metal oxide semiconductors. Increasing the alkyl chain length reduces surface energy and imparts hydrophobic properties to the surface. Additionally, it lowers the threshold voltage by reducing trap states in oxide layers and increases carrier mobility. SAM materials contribute to aligning the energy difference between the work function of the metal oxide buffer layer and the highest-occupied molecular orbital (HOMO) or lowest-unoccupied molecular orbital (LUMO) energy levels of the organic material. However, to our knowledge, comprehensive analyses of the diode parameters and charge transport characteristics of metal/SAMs/TiO_2-based Schottky diodes are rare in literature. Although there exists research focused on modulating the Schottky barrier by incorporating SAMs at the Pt/TiO_2 interface, detailed investigations into these aspects are limited [33-37]. To enhance the performance of next-generation Schottky diodes, a detailed investigation of the effects of SAM molecules is required. In the study conducted by Can and Havare (2022), the MZ187 molecule demonstrated excellent electronic properties due to its strong π-conjugation, making it a promising candidate for organic semiconductor applications. When employed as a SAM in OLED devices, MZ187 was found to enhance charge transport and reduce interface trap states. This capability has inspired its integration into Schottky diode structures, where its role in modifying the interface properties can lead to improved diode performance, particularly in terms of reducing R_s and increasing $\varnothing_b$ [38].

This study explores the influence of SAMs on the electrical properties and charge transport behavior of Schottky diodes in an Al/SAM/TiO_2/p-Si structure. Our research reveals the impact of SAMs on key parameters such as *n*, R_s, and $\varnothing_b$. We demonstrated how SAMs enhance the performance of Schottky diodes, contributing to the advancement of nano electronic devices.

II. EXPERIMENTAL SECTION

A. Materials: Ammonium hydroxide (NH_4OH), hydrogen peroxide (H_2O_2), hydrofluoric acid (HF), titanium (IV) isopropoxide ($Ti(OC_3H_7)_4$), trimethylamine (C_3H_9N), acetic acid (CH_3COOH), acetonitrile (CH_3CN), and ethanol (C_2H_5OH) obtained from Sigma-Aldrich.

B. Sol-gel TiO_2 preparation: The TiO_2 solution was prepared using the sol-gel method, following the steps detailed in our previous research [39]. Titanium (IV) isopropoxide was gradually added to ethanol and mixed at room temperature for one hour to initiate hydrolysis and condensation reactions. Subsequently, acetic acid and trimethylamine were added to the solution in ethanol to adjust the pH and control the nucleation and growth of TiO_2 particles. The solution was then mixed for three hours to ensure thorough mixing and homogeneity of the components. The solution was left to age overnight, allowing further condensation reactions to occur and improving the homogeneity and stability of the resulting TiO_2 solution.

C. 4", 4""-[biphenyl-4,4" -diylbis(phenylimino)]dibiphenyl-4-carboxylic acid (MZ187) Synthesis: The synthesis steps of the molecule are detailed in the OLED study by Can and Havare [38].

D. Schottky Diode Fabrication: The diode in the Al/SAMs/TiO_2/p-Si configuration was produced on the p-type silicon substrate with a resistivity of 5-10 Ωcm. The front surface of the silicon substrates was cleaned using the RCA cleaning procedure, which includes oxide removal, organic cleaning, and ionic cleaning steps [40]. Initially, the substrates were subjected to an NH_4OH:H_2O_2:H_2O (1:1:6) solution to eliminate organic impurities and followed by a 10 minutes heating period. Subsequently, a 30 second treatment with HF:10H_2O was employed to remove the SiO_2 layer. The substrates were then immersed in an HCl + H_2O_2 + 6H_2O solution for 10 minutes. After each step, the Si substrates were dried with N_2 gas. Before the TiO_2 deposition, a 1200 Å layer of aluminum (Al) with 99.999% purity was thermally evaporated onto the back side of the Si substrate in a 10^{-6} Torr vacuum environment. The substrates were subjected to annealing at 570°C for 5 minutes in a nitrogen atmosphere to form an ohmic back contact with low resistance. This step was crucial for optimizing the electrical contact between the metal and the semiconductor, ensuring effective charge carrier transport and reducing contact resistance. The TiO_2 layer was applied to the substrates by spin coating at 2000 rpm for 30 seconds and then annealed at 450°C for 1 hour to obtain a thin TiO_2 film in anatase phase [41,42]. The TiO_2-coated substrates were immersed for 24 hours in a solution of MZ187 prepared by dissolving in acetonitrile at a concentration of 1 mM at room temperature. Finally, using a shadow mask, a 100 nm Al metal was deposited onto the top surface of the MZ187 molecules under high vacuum conditions (10^{-6} Torr).

E. Characterization: The electrical characteristics of the Schottky diodes were evaluated by performing the current-voltage (*I–V)* measurements with a Keithley 2400 source meter across a voltage range of -2 to 2 V. These measurements were carried out at ambient temperature and under dark conditions. The TiO_2 film thickness was measured via the Ambios P7 profilometer. Capacitance-voltage (*C*-*V*) measurements were carried out using a Keithley 4200 system, measuring the device capacitance across an applied voltage sweep from -2 V to 2 V.

III. RESULTS AND DISCUSSION

The *I*-*V* characteristics of Schottky diodes with/without MZ187 are presented on a semi-logarithmic scale in Figure 1a. The device architecture is shown in Figure 1b. As expected, the diodes exhibited good rectifying behavior, with current increasing linearly with voltage at low forward bias voltages. However, at higher voltages, this linear relationship was disrupted due to the presence of R_s and interface layers, leading to the formation of interface states. The deviation from linearity at elevated voltages is primarily due to the increasing influence of R_s and interface layers within the device. These resistance components become more pronounced under higher applied voltages, resulting in the emergence of interface states and adversely affecting the device performance [43]. Understanding these mechanisms is crucial for developing high-performance Schottky diodes, as it highlights the limitations imposed by interface effects and resistance losses. The current flow in these devices is influenced by various factors. These include the temperature variations, semiconductor fabrication parameters, applied forward bias, and the presence of insulating layers. Different theoretical models, such as thermionic emission (TE), Cheung-Cheung, and Norde functions, have been proposed to explain the charge transport mechanisms of Schottky diodes. According to TE theory, the *I-V* characteristics of MIS contacts are described by the relationship between the current and the applied forward bias, as given by Equation 1 [3,44,45].

$$I = I_0\left(\exp\left(\frac{qV}{nkT}\right) - 1\right) \tag{1}$$

$$I_0 = AA^*T^2\exp\left(-\frac{q\emptyset_{b0}}{kT}\right) \tag{2}$$

Here, I_0 is the reverse saturation current, q is the electron charge, k is the Boltzmann constant, n is the ideality factor indicating how close the diode is to ideal behavior (n=1), A is the rectifying contact area (7.85x10^{-3} cm^2), T is the temperature, and A* is the effective Richardson constant (32 A/cm^{2}K^2 for p-Si). Additionally, $\emptyset_{b0}$: the barrier height at zero forward bias, and the relationship is given by:

$$\emptyset_{b0} = \frac{kT}{q}\ln\left(\frac{AA^*T^2}{I_0}\right) \tag{3}$$

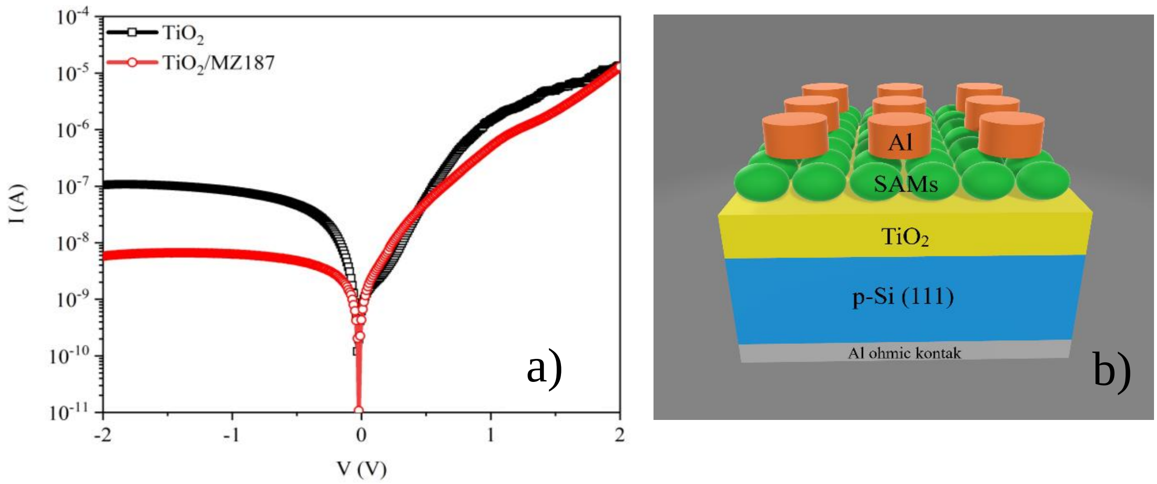

Figure 1. ***(a)*** *I-V characteristics of the Schottky diodes, and* ***(b)*** *the diode configuration fabricated with MZ187.*

The n can be derived from the following Equation 4, which considers the slope of the *lnI-V* in the forward bias region (for V>3kT/q):

$$n = \frac{q}{kT}\frac{\mathrm{d}V}{\mathrm{d}(\ln I)} \tag{4}$$

The n values calculated from the *lnI-V* graphs for the control and MZ187-modified TiO_2-based diodes are 3.7 and 2.7 at room temperature, respectively. This indicates that the MZ187-modified diodes exhibit a more ideal diode behavior. Deviations from ideality can be attributed to factors such as R_s, N_{ss}, and interface insulation layers. The rectification ratios (IF/IR) derived from the *I-V* in the range of +2V to -2V are 1.3x10^2 for the control diode and 2.2x10^3 for the MZ187-modified diode, demonstrating an improvement in the rectification ratio with MZ187 compared to the control diode.

To calculate the Schottky barrier height $\emptyset_{b0}$, the reverse saturation current I_0 can be used. First, the I_0 are obtained from the intersection of the *lnI-V* curves under zero forward bias conditions, which are

$3.5x10^{-9}$ A for the control diode and $1.2x10^{-9}$ A for the MZ187-based diode. This indicates that MZ187 reduces the reverse saturation current, resulting in lower leakage current. Subsequently, $\O_{b0}$ can be determined by substituting I_0 into Equation 3. The values of $\O_{b0}$ for the control and MZ187-based diodes are obtained to be 0.76 eV and 0.79 eV, respectively. These results show that MZ187 enhances the barrier height, thereby improving the overall performance of the device [27,46,47].

As known, the forward *I-V* characteristics of Schottky diodes can exhibit significant non-ideal behavior at high voltage regions due to factors such as R_s. The R_s is influenced by the presence of the semiconductor/metal interface and leads to non-ideal diode characteristics. The method developed by Cheung-Cheung is highly effective in determining R_s, and this method can be used to find the Schottky diode parameters $\O_b$ and n. The Cheung-Cheung functions are as follows:[48]

$$I = I_0 \exp\left(\frac{q(V-IR_s}{nkT}\right) \tag{5}$$

$$\frac{\mathrm{d}V}{\mathrm{d}(lnI)} = IR_s + n\left(\frac{kT}{q}\right) \tag{6}$$

$$H(I) = V - n\frac{kT}{q}\ln\left(\frac{I}{AA^*T^2}\right) \tag{7}$$

$$H(I) = IR_s + n\emptyset_B \tag{8}$$

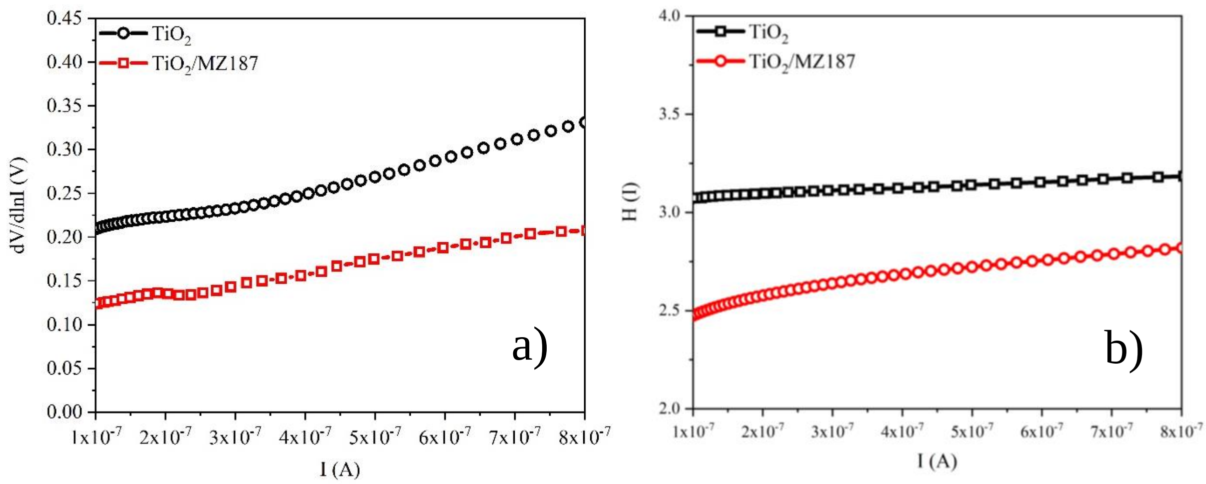

Figure 2. (a) *dV/dLnI(V)-I (A) and* ***(b)*** *H(I)-I graphs of Schottky diodes.*

The n values derived from Equation 6 for the control and the MZ187-modified TiO_2 diode at room temperature are 4.4 and 2.8, respectively. The slope of the linear graph obtained from Equation 6 allows us to calculate R_s. The calculated R_s values for the control and MZ187-based diodes are 168.3 kΩ and 129.2 kΩ, respectively. The decrease in R_s with the MZ187 molecule indicates that passivation has occurred at the Al/TiO_2 interface. From the linear fit of the *H(I)-I* graph, plotted using Equation 8, the y-intercept provides the $\O_b$ value, while the slope gives R_s. The R_s calculated from the *H(I)-I* graph for the control and MZ187-based diodes are 90.3 kΩ and 76.1 kΩ, respectively, demonstrating that MZ187 reduces the series resistance and improves the device performance. The $\O_b$ values are 0.80 eV for the control diode and 0.82 eV for the MZ187-based diode (Figure 2). These findings indicate that MZ187 not only decreases the series resistance but also increases the barrier height, thereby enhancing the overall performance of the Schottky diodes [49,50].

Another important method for calculating $\O_b$ and R_s is the Norde method. The Norde functions expressed based on *I-V* measurements are as follows:[51]

$$F(V) = \frac{V}{\gamma} - \frac{kT}{q}\ln\left(\frac{I}{AA^{*}T^{2}}\right) \tag{9}$$

$$\emptyset_b = F(V_0) + \frac{V_0}{\gamma} - \frac{kT}{q} \tag{10}$$

$$R_s = \frac{kT(\gamma - n)}{qI_{min}(V_0)} \tag{11}$$

Here, γ is a random integer greater than n. V is the voltage and I represent the current obtained from the I-V measurements. After determining the γ values as 4 for the control and 3 for the MZ187-based diodes, the $F(V)$-V plot can be constructed. From the $F(V)$-V plot in Figure 3, the diode barrier heights $\emptyset_b$ can be calculated by substituting the values corresponding to the minimum $F(V_0)$ at the lowest voltage V_0 into the equation. The $\emptyset_b$ values calculated from Equation 10 are 0.78 eV for the control and 0.80 eV for the MZ187-based diodes. The R_s values calculated from Equation 11 are 5.5 MΩ for the control and 3.5 MΩ for the MZ187-based diodes. Both analytical methods demonstrate that the MZ187 molecule effectively improves the performance of Schottky diodes. The decrease in R_s values for MZ187-based diodes indicates surface passivation, resulting in reduced resistance to current conduction. Additionally, the increase in $\emptyset_b$ values suggests that these diodes offer a higher barrier height and consequently lower leakage current [52].

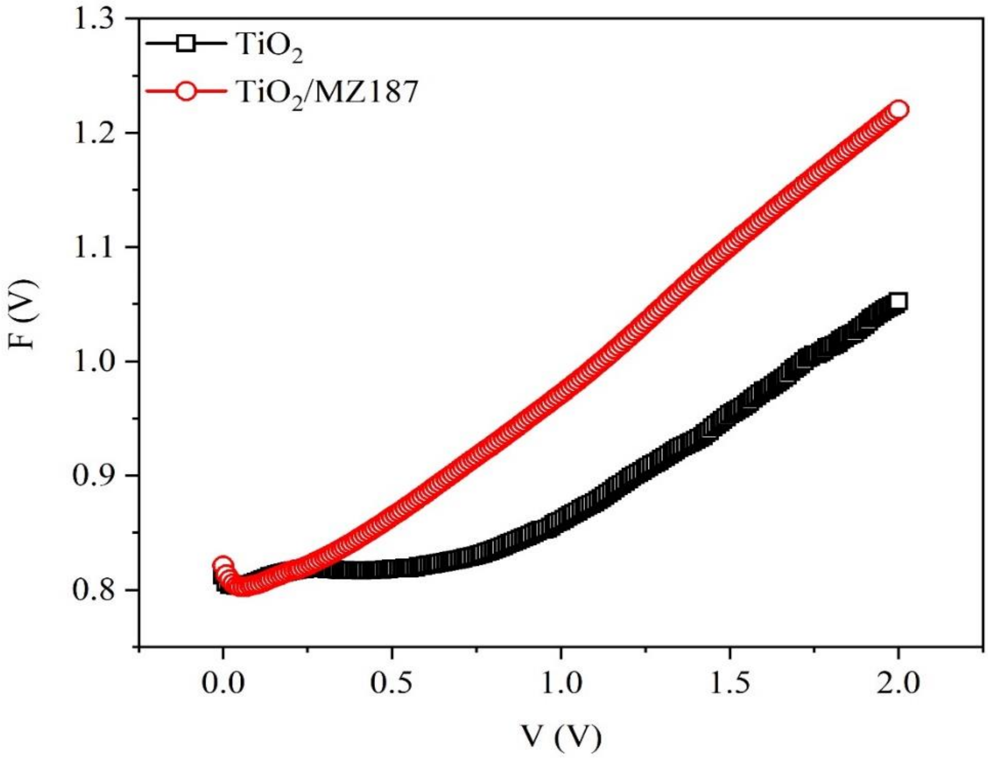

Figure 3. *F(V)-V plots of Schottky diodes.*

It is evident that the Schottky diode parameters obtained using the three different methods vary significantly from one another. The Norde method assumes an ideal metal/semiconductor contact and typically considers the ideality factor n=1. This method collects data from the linear region of the I-V, where the current changes exponentially. As a result, R_s values calculated using the Norde method are 5.5 MΩ for the control and 3.5 MΩ for the MZ187-based diodes. In contrast, the Cheung-Cheung method uses data from the nonlinear regions of the I-V, accounting for R_s and determining $\emptyset_b$ values. This method considers interface effects and free carriers but may yield different results due to the indirect evaluation of these effects. For the Cheung-Cheung method, R_s values are calculated as 168.3 kΩ for the control and 129.2 kΩ for the MZ187-based diodes. The $\emptyset_b$ values are 0.78 eV and 0.80 eV for the Norde method and 0.80 eV and 0.82 eV for the Cheung-Cheung method, respectively. These differences arise from the different regions of the *lnI-V* graph from which each method collects data. As shown in Table 1, there are significant variations in the R_s obtained using the three methods. The R_s values obtained from the Norde method may differ from those obtained using the Cheung-Cheung and *I-V* technique. Furthermore, difficulties in accurately identifying the minimum points of the *F(V)-V* curves can introduce error margins. The Norde method, which derives the R_s from the linear region of the *lnI-V* characteristics, and accurately identifying the turning points of the graph is critical for calculating R_s correctly. Consequently, the differences between methods are due to the regions of data analysis and the assumptions used [3,53,54].

Table 1. *Electrical parameters of Schottky diodes obtained using different methods.*

Device parameters	**TiO_2**	**TiO_2/MZ187**
n *(I-V)*	3.7	2.7
n *(dV/dln(I)) (kΩ)*	4.4	2.8
I_0 (A)	$3.5x10^{-9}$	$1.2x10^{-9}$
∅ (I-V) eV	0.76	0.79
∅ (H-V) eV	0.80	0.82
∅ (F-V) eV	0.78	0.80
R_s *(dV/dln(I)) (kΩ)*	168.3	129.2
R_s *(H(I)-I) (kΩ)*	90.3	76.1
R_s *(F(V)-V) (MΩ)*	5.5	3.5
Rectification ratio	$1.3x10^2$	$2.2x10^3$

The experimental findings presented in this study are in good agreement with the electrical parameters observed in similar Schottky diode structures reported in Table 2. The calculated parameters such as ideality factor and series resistance exhibit comparable trends, strengthening the consistency of the results obtained with the results obtained from previous studies on TiO_2-based Schottky diodes fabricated with different deposition techniques.

***Table 2**. Comparison of electrical parameters in Schottky diodes with TiO_2 fabricated using various deposition techniques.*

Deposition Method	**Structure**	**T *(K)***	**n**	**$\emptyset_b$ *(eV)***	**Ref.**
ALD	Au/TiO_2/n-4H-SiC	300	-	1.068 (100 kHz), 0.347 (1 MHz)	[21]
ALD	TiO_2 Interlayer/4H-SiC	300	-	0.63-0.90	[25]
ALD	Al/TiO_2/p-Si	300	1.8	0.66	[20]
DC Magnetron Sputtering	Au/TiO_2 (rutile)/n-Si	200-380	3.50-1.9	0.57-0.82	[18]
DC Magnetron Sputtering	Au/TiO_2 (anatase)/n-Si	340-400	2.47-2.24	0.74-0.85	[19]
DC Magnetron Sputtering	Ag/TiO_2/n-InP	300	1.39 (60 Å), 1.41 (120 Å)	0.50-0.52	[24]
Electrochemical Anodization	Ag/TiO_2 nanotube/Ti	300	2.39	0.92	[22]
Electrochemical Anodization	Pt/TiO_2 nanotubes/Ti	300	1.25	0.91	[26]
Sol-Gel/Drop Casting	Al/Zr-doped TiO_2/p-Si	300	2.39	-	[23]
Sol-Gel/Spin coating	**A/SAMs/TiO_2/p-Si**	**300**	**2.7**	**0.79**	**this work**

The electrical properties of Schottky barrier diodes can vary significantly based on the interaction between the interfacial layer's thickness and the N_{ss} at the metal-semiconductor junction. N_{ss} is a critical factor that directly influences the diode's overall performance and quality, particularly affecting the n and $\varnothing_b$. The distribution of N_{ss} can be derived from the forward-bias I-V of the diode. The voltage dependence of N_{ss} can be mathematically described using the following Equation 12:[9,55,56]

$$N_{ss}(V) = \frac{1}{q}\left[\frac{\varepsilon_i}{d}(n(V)-1) - \frac{\varepsilon_s}{W_d}\right] \tag{12}$$

Here, N_{ss} represents the density of surface states at equilibrium with the semiconductor, W_d denotes the width of the depletion region, ε_s is the permittivity of the semiconductor, ε_i is the permittivity of the interfacial layer, n is the ideality factor, d is the thickness of the insulating layer. The TiO_2 thin film's thickness was measured at 53 nm using a profilometer. The expression for W_d can be written as:[40]

$$W_D = \left[\frac{2\varepsilon_0\varepsilon_s V_0}{qN_A}\right]^{\frac{1}{2}} \tag{13}$$

where $\varepsilon_s=11.8\varepsilon_0$, and V_0 represents the built-in potential, which is determined by extrapolating the $1/C^2$–V curve onto the voltage axis as shown in Figure 4. Analysis of the $1/C^2$–V characteristic at 500 kHz yields a slope that corresponds to an acceptor density (N_A) of $2.7\text{x}10^{17}$ cm^{-3} within the semiconductor. The calculated W_d is 63 nm. Extrapolation of this curve on the voltage axis allows for the determination of the V_0. This capacitance relation is represented by:[45]

$$C^{-2} = \frac{2(V_0+V)}{\varepsilon_0\varepsilon_s qA^2N_A} \tag{14}$$

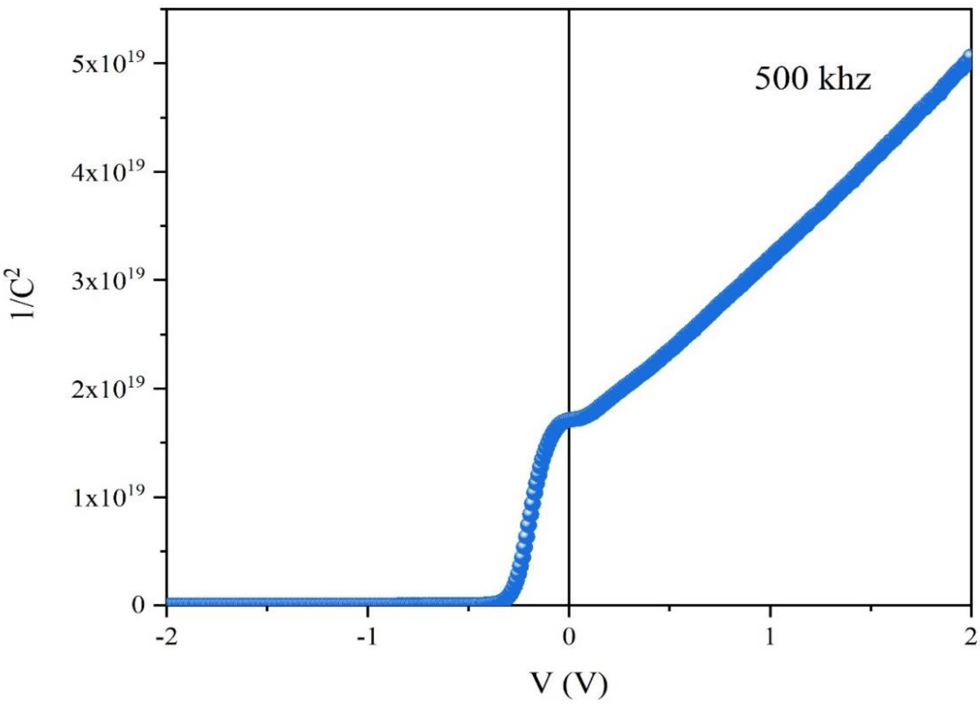

***Figure 4**. $1/C^2$–V characteristics of the Schottky diode with MZ187 at 500 kHz.*

For p-type semiconductors, the energy of the surface states (E_{ss}) with respect to the valence band maximum of the semiconductor is given by:

$$\varnothing_e = \varnothing_{bo} + \beta(V - IR_s) = \varnothing_{bo} + \left(\frac{1}{1-n(V)}\right)(V - IR_s) \tag{15}$$

$$E_{ss} - E_v = q[\emptyset_e - (V - IR_s)] \tag{16}$$

Here, V represents the applied voltage drop, $\emptyset_e$ is the effective barrier height. Using Equation (12), N_{ss} as a function of voltage can be determined. As shown in Figure 5, N_{ss} decreases as $E_v - E_{ss}$ increases. Clearly, the use of the MZ187 molecule has led to a reduction in N_{ss}. The observed decrease in N_{ss} indicates a reduction in trap states at the Al/TiO_2 interface in the MZ187-modified diodes [9,57]. The reduction of trap states enhances the device's performance and stability, as trap states can negatively impact electrical parameters and lead to carrier recombination [58,59]. These results highlight the potential of SAMs to improve interface quality and enhance the electrical properties of Schottky barrier diodes.

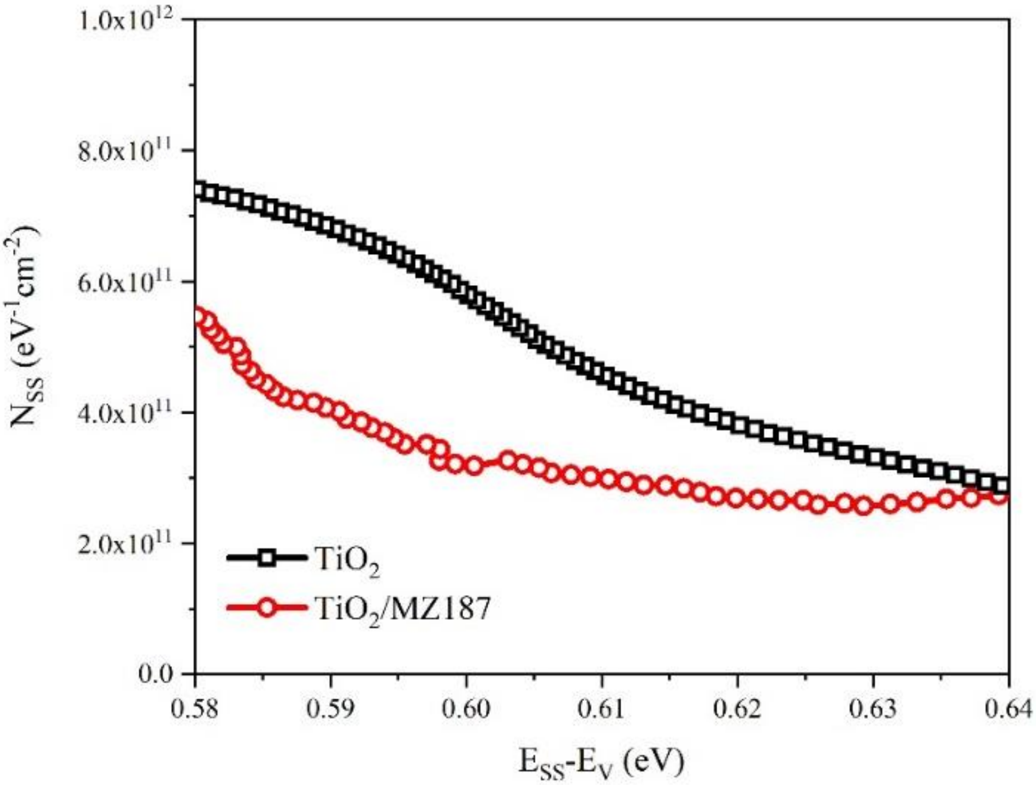

Figure 5. *N_{ss} as a function of E_{ss}-E_v for the Schottky diodes at room temperature.*

III. CONCLUSION

In this study, the electrical properties and charge transport mechanisms of Schottky barrier diodes fabricated using the MZ187 molecule were examined. The results demonstrate that the MZ187 molecules enhance the Schottky diode performance. Compared to the control diode, the n values for MZ187-based diode decreased from 3.7 to 2.7. The R_s values, calculated using various methods, significantly decreased in the MZ187-modified diode, indicating that the MZ187 molecules improves surface quality. The application of the MZ187 molecule resulted in an increase in $\emptyset_b$. The rectification ratio of the control diode was $1.3x10^2$, while for the MZ187-coated diode, this ratio increased to $2.2x10^3$. This improvement was achieved by reducing localized interface states at the metal/semiconductor interfaces due to MZ187 molecules. The findings of this study indicate that SAM coatings are an effective method for improving Schottky diode performance. The use of SAM molecules holds potential for enhancing the efficiency and stability of nano-electronic devices. Our research contributes to the development of nano-electronic devices by revealing the effects of SAMs on key parameters such as rectification ratios, R_s, n, and $\emptyset_b$. Additionally, exploring the combinations of SAM molecules with different metal oxides and semiconductors will be a crucial step towards developing higher performance and more stable devices.

IV. REFERENCES

[1] A. J. King, A. Z. Weber, and A. T. Bell, “Theory and simulation of metal-insulator-semiconductor (MIS) photoelectrodes,” *ACS Appl Mater Interfaces*, vol. 15, no. 19, pp. 23024–23039, 2023.

[2] S. Zeyrek, “The effect of interface states and series resistance on current-voltage characteristics in (MIS) schottky diodes,” *Afyon Kocatepe University Journal of Sciences and Engineering*, vol. 15, no. 2, pp. 1–9, 2015.

[3] S. M. Sze and Kwok K. Ng, *Physics of Semiconductor Devices Third Edition*, New Jersey, USA, John Wiley & Sons, Inc., 2007, pp. 90-96.

[4] Ç. Ş. Güçlü, “A comparison electronic specifications of the ms & mps type Schottky diodes (SDS) via utilizing voltage-current (V-I) characteristics,” *Gazi University Journal of Science Part A: Engineering and Innovation*, vol. 10, no. 1, pp. 62–69, 2023.

[5] M. Soylu, I. S. Yahia, F. Yakuphanoglu, and W. A. Farooq, “Modification of electrical properties of al/p-si Schottky barrier device based on 2′-7′-dichlorofluorescein,” *J Appl Phys*, vol. 110, no. 7, pp. 074514, 2011.

[6] S. S. Fouad, G. B. Sakr, I. S. Yahia, D. M. Abdel-Basset, and F. Yakuphanoglu, “Capacitance and conductance characterization of nano-ZnGa 2Te4/n-si diode,” *Mater Res Bull*, vol. 49, no. 1, pp. 369–383, 2014.

[7] Ö. Vural, Y. Şafak, A. Türüt, and Ş. Altindal, “Temperature dependent negative capacitance behavior of Al/rhodamine-101/n- GaAs Schottky barrier diodes and R s effects on the C-V and G/ω-V characteristics,” *J Alloys Compd*, vol. 513, pp. 107–111, 2012.

[8] K. Shili, M. Ben Karoui, R. Gharbi, M. Abdelkrim, M. Fathallah, and S. Ferrero, “Series resistance study of Schottky diodes developed on 4H-SiC wafers using a contact of titanium or molybdenum,” *Microelectron Eng*, vol. 106, pp. 43–47, 2013.

[9] O. Pakma, N. Serin, T. Serin, and Ş. Altndal, “On the energy distribution profile of interface states obtained by taking into account of series resistance in Al/TiO2/pSi (MIS) structures,” *Physica B Condens Matter*, vol. 406, no. 4, pp. 771–776, 2011.

[10] Gyanan, S. Mondal, and A. Kumar, “Tunable dielectric properties of TiO2 thin film based MOS systems for application in microelectronics,” *Superlattices Microstructures*, vol. 100, pp. 876–885, 2016.

[11] G. Zerjav, K. Zizek, J. Zavasnik, and A. Pintar, “Brookite vs. rutile vs. anatase: What’s behind their various photocatalytic activities?,” *J Environ Chem Eng*, vol. 10, no. 3, pp. 107722, 2022.

[12] R. Agarwal, Himanshu, S. L. Patel, S. Chander, C. Ameta, and M. S. Dhaka, "Understanding the physical properties of thin TiO2 films treated in different thermal atmospheric conditions," *Vacuum*, vol. 177, pp. 109347, 2020.

[13] J. Buckeridge *et al.*, "Polymorph engineering of Tio2: demonstrating how absolute reference potentials are determined by local coordination," *Chemistry of Materials*, vol. 27, no. 11, pp. 3844–3851, 2015.

[14] S.-D. Mo and W. Y. Ching, "Electronic and optical properties of three phases of titanium dioxide: Rutile, anatase, and brookite," *Physical Review B*, Vol. 51, no. 19, pp. 13023-13032, 1994.

[15] W. Promnopas *et al.*, "Crystalline phases and optical properties of titanium dioxide films deposited on glass substrates by microwave method," *Surf Coat Technol*, vol. 306, pp. 69–74, 2016.

[16] D. Bokov *et al.*, "Nanomaterial by sol-gel method: synthesis and application," *Advances in Materials Science and Engineering*, Vol. 2021, Issue 1, pp. 5102014, 2021.

[17] O. Pakma, N. Serin, T. Serin, and Ş. Altindal, "The double Gaussian distribution of barrier heights in Al/ TiO 2/p-Si (metal-insulator-semiconductor) structures at low temperatures," *J Appl Phys*, vol. 104, no. 1, pp. 014501, 2008.

[18] B. Kinaci, S. Şebnem Çetin, A. Bengi, and S. Özçelik, "The temperature dependent analysis of Au/TiO2 (rutile)/n-Si (MIS) SBDs using current-voltage-temperature (I-V-T) characteristics," *Mater Sci Semicond Process*, vol. 15, no. 5, pp. 531–535, 2012.

[19] B. Kinaci, T. Asar, Y. Özen, and S. Özçelik, "The analysis of Au/Ti02/n-Si Schottky barrier diode at high temperatures using I-V characteristics," O*ptoelectronics and Advanced Materials-rapid Communications*, vol. 5, no. 4, pp. 434–437, 2011.

[20] S. B. K Aydin, I. E. Yildiz, and I. Kanbur Çavu, "ALD TiO 2 thin film as dielectric for Al/p-Si Schottky diode,"*Bulletin of Materials Science*, Vol. 37, pp. 1563-1568, 2014.

[21] E. E. Tanrikulu, D. E. Yildiz, A. Günen, and Altindal, "Frequency and voltage dependence of electric and dielectric properties of Au/TiO2/n-4H-SiC (metal-insulator-semiconductor) type Schottky barrier diodes," *Phys Scr*, vol. 90, no. 9, pp. 095801, 2015.

[22] M. Yilmaz, B. B. Cirak, S. Aydogan, M. L. Grilli, and M. Biber, "Facile electrochemical-assisted synthesis of TiO2 nanotubes and their role in Schottky barrier diode applications," *Superlattices Microstructures*, vol. 113, pp. 310–318, 2018.

[23] İ. H. Taşdemir, Ö. Vural, and İ. Dökme, "Electrical characteristics of p-Si/TiO2/Al and p-Si/TiO2-Zr/Al Schottky devices," *Philosophical Magazine*, vol. 96, no. 16, pp. 1684–1693, 2016.

[24] A. Kürşat Bilgili, R. Çağatay, M. K. Öztürk, and M. Özer, “Investigation of electrical and structural properties of Ag/TiO 2 /n-InP/Au Schottky diodes with different thickness TiO 2 interface”, *Silicon*, Vol. 14, pp. 3013-3018, 2022.

[25] B. Y. Tsui, J. C. Cheng, L. S. Lee, C. Y. Lee, and M. J. Tsai, “Schottky barrier height modification of metal/4H-SiC contact using ultrathin TiO2 insertion method,” *Japanese Journal of Applied Physics*, Vol. 53, pp. 04EP10, 2014.

[26] L. B. Taşyürek, “Synthesis of TiO2 nanotubes and photodiode performance,” *Türk Doğa ve Fen Dergisi*, vol. 12, no. 3, pp. 72–77, 2023.

[27] A. M. Nawar, M. Abd-Elsalam, A. M. El-Mahalawy, and M. M. El-Nahass, “Analyzed electrical performance and induced interface passivation of fabricated Al/NTCDA/p-Si MIS–Schottky heterojunction,” *Appl Phys A Mater Sci Process*, vol. 126, no. 113, 2020.

[28] F. Yakuphanoglu, S. Okur, and H. Özgener, “Modification of metal/semiconductor junctions by self-assembled monolayer organic films,” *Microelectron Eng*, vol. 86, no. 11, pp. 2358–2363, 2009.

[29] Z. Çaldıran, “Modification of Schottky barrier height using an inorganic compound interface layer for various contact metals in the metal/p-Si device structure,” *J Alloys Compd*, vol. 865, pp. 158856, 2021.

[30] G. Güler, Ö. Güllü, Ş. Karataş, and Ö. F. Bakkalolu, “Analysis of the series resistance and interface state densities in metal semiconductor structures,” *J Phys Conf Ser*, vol. 153, pp. 012054, 2009.

[31] I. M. Afandiyeva, S. Altındal, L. K. Abdullayeva, and A. I. Bayramova, “Self-assembled patches in PtSi/n-Si (111) diodes,” *Journal of Semiconductors*, vol. 39, no. 5, pp. 054002, 2018.

[32] M. Can *et al.*, “Electrical properties of SAM-modified ITO surface using aromatic small molecules with double bond carboxylic acid groups for OLED applications,” *Appl Surf Sci*, vol. 314, pp. 1082–1086, 2014.

[33] S. Kim and H. Yoo, “Self-assembled monolayers: Versatile uses in electronic devices from gate dielectrics, dopants, and biosensing linkers,” *Micromachines,* Vol. 12 (5), pp. 565, 2021.

[34] Z. R. Lan, J. Y. Shao, and Y. W. Zhong, “Self-assembled monolayers as hole-transporting materials for inverted perovskite solar cells,” *Mol. Syst. Des. Eng.*, Vol. 8, pp. 1440-1455, 2023.

[35] S. H. Hsiao, J. X. Wu, and H. I. Chen, “High-selectivity NOx sensors based on an Au/InGaP Schottky diode functionalized with self-assembled monolayer of alkanedithiols,” *Sens Actuators B Chem*, vol. 305, pp. 127269, 2020.

[36] B. De Boer, A. Hadipour, M. M. Mandoc, T. Van Woudenbergh, and P. W. M. Blom, "Tuning of metal work functions with self-assembled monolayers," *Advanced Materials*, vol. 17, no. 5, pp. 621–625, 2005.

[37] Y. Liu, D. Ji, and W. Hu, "Recent progress of interface self-assembled monolayers engineering organic optoelectronic devices," *DeCarbon*, vol. 3, p. 100035, 2024.

[38] M. Can and A. K. Havare, "OLED application of π-conjugated phenylimino carboxylic acid organic semiconductor material," *EPJ Applied Physics*, vol. 97, no. 33, pp.8, 2022.

[39] C. Tozlu, A. Mutlu, M. Can, A. K. Havare, S. Demic, and S. Icli, "Effect of TiO 2 modification with amino-based self-assembled monolayer on inverted organic solar cell," *Appl Surf Sci*, vol. 422, pp. 1129–1138, 2017.

[40] Western Kern, *Handbook of Semiconductor Wafer Cleaning Technology*, New Jersey, USA, pp. 253-256, 1993.

[41] H. Noh, S. G. Oh, and S. S. Im, "Preparation of anatase TiO 2 thin film by low temperature annealing as an electron transport layer in inverted polymer solar cells," *Appl Surf Sci*, vol. 333, pp. 157–162, 2015.

[42] M. Shahiduzzaman *et al.*, "Low-temperature treated anatase TiO2 nanophotonic-structured contact design for efficient triple-cation perovskite solar cells," *Chemical Engineering Journal*, vol. 426, pp. 131831, 2021.

[43] O. Pakma, N. Serin, T. Serin, and Ş. Altndal, "On the energy distribution profile of interface states obtained by taking into account of series resistance in Al/TiO2/pSi (MIS) structures," *Physica B Condens Matter*, vol. 406, no. 4, pp. 771–776, 2011.

[44] E. H. Rhoderick and R. H. Williams, *Metal-Semiconductor Contacts Second Edition*, Clarendon Press, Oxford, pp. 89-109, 1988.

[45] B. Akın, M. Ulusoy, and S. Altındal Yerişkin, "Investigation of the interface state characteristics of the Al/Al2O3/Ge/p-Si heterostructure over a wide frequency range by capacitance and conductance measurements," *Mater Sci Semicond Process*, vol. 170, pp. 107951, 2024.

[46] H. J. Lee, W. A. Anderson, H. Hardtdegen, and H. Lilth, "Barrier height enhancement of Schottky diodes on n- In0.53Ga0.47As by cryogenic processing," *Appl. Phys. Lett.*, Vol. 63, 1939–1941, 1993.

[47] A. D. Marwick, M. O. Aboelfotoh, and R. Casparis, "Increase in Schottky barrier height in the CoSi 2 /Si (100) interface caused by hydrogen." *Mrs Online Proceeding Library*, Vol. 281, pp. 629-634, 1992.

[48] S. K. Cheung and N. W. Cheung, "Extraction of Schottky diode parameters from forward current-voltage characteristics," *Appl Phys Lett*, vol. 49, no. 2, pp. 85–87, 1986.

[49] S. Y. Yu, D. C. Huang, Y. L. Chen, K. Y. Wu, and Y. T. Tao, "Approaching charge balance in organic light-emitting diodes by tuning charge injection barriers with mixed monolayers," *Langmuir*, vol. 28, no. 1, pp. 424–430, 2012.

[50] G. S. Kim, S. H. Kim, J. Park, K. H. Han, J. Kim, and H. Y. Yu, "Schottky barrier height engineering for electrical contacts of multilayered MoS2 transistors with reduction of metal-induced gap states," *ACS Nano*, vol. 12, no. 6, pp. 6292–6300, 2018.

[51] H. Norde, "A modified forward I-V plot for Schottky diodes with high series resistance," *J Appl Phys*, vol. 50, no. 7, pp. 5052–5053, 1979.

[52] G. Çankaya and N. Uçar, "Schottky barrier height dependence on the metal work function for p-type si Schottky diodes," *Z. Naturforsch.*, Vol. 59a, pp. 795-798, 2004.

[53] D. A. Aldemir, A. Kökce, and A. F. Özdemir, "Schottky diyot parametrelerini belirlemede kullanılan metotların geniş bir sıcaklık aralığı için kıyaslanması," *SAÜ Fen Bilimleri Enstitüsü Dergisi*, Vol. 21, Issue 6, pp. 1286-1292, 2017.

[54] S. Hameed, Ö. Berkün, and S. Altındal Yerişkin, "On the voltage dependent series resistance, interface traps, and conduction mechanisms in the Al/(Ti-doped dlc)/p-si/Au Schottky barrier diodes (SBDs)," *Gazi University Journal of Science Part A: Engineering and Innovation*, vol. 11, no. 1, pp. 235–244, 2024.

[55] H. C. Card and E. H. Rhoderick, "Studies of tunnel MOS diodes I. Interface effects in silicon Schottky diodes," *J. Phys. D: Appl. Phys.*, Vol. 4, pp. 1589, 1971.

[56] S. ALTINDAL YERİŞKİN, "Effects of (0.01Ni-PVA) interlayer, interface traps (Dit), and series resistance (Rs) on the conduction mechanisms(CMs) in the Au/n-Si (MS) structures at room temperature," *Iğdır Üniversitesi Fen Bilimleri Enstitüsü Dergisi*, vol. 9, no. 2, pp. 835–846, 2019.

[57] D. E. Yildiz, Ş. Altindal, Z. Tekeli, and M. Özer, "The effects of surface states and series resistance on the performance of Au/SnO2/n-Si and Al/SnO2/p-Si (MIS) Schottky barrier diodes," *Mater Sci Semicond Process*, vol. 13, no. 1, pp. 34–40, 2010.

[58] I. Taşçıoğlu, G. Pirgholi-Givi, S. A. Yerişkin, and Y. Azizian-Kalandaragh, "Examination on the current conduction mechanisms of Au/n-Si diodes with ZnO–PVP and ZnO/Ag2WO4 –PVP interfacial layers," *J Solgel Sci Technol*, vol. 107, no. 3, pp. 536–547, 2023.

[59] Ç. Ş. Güçlü, "On the impact of pure PVC and (PVC: Ti) interlayer on the conduction mechanisms and physical parameters of classic metal-semiconductor (MS) Schottky diodes (SDs)," *Physica B: Condensed Matter*, Vol. 689, pp. 416173, 2024.